Melting Behavior, Isothermal and Nonisothermal Crystallization Kinetics of PP/mLLDPE Blends

Jianglei Qin, Shaoqiang Guo, Zhiting Li

College of Chemistry and Environmental Science, Hebei University, Baoding 071002, China

Received 20 August 2007; accepted 14 February 2008
DOI 10.1002/app.28214
Published online 18 April 2008 in Wiley InterScience (www.interscience.wiley.com).

ABSTRACT: Melting behavior, nonisothermal crystallization and isothermal crystallization kinetics of polypropylene (PP) with metallocene-catalyzed linear low density polyethylene (mLLDPE) were studied by differential scanning calorimetry (DSC). The results show that PP and mLLDPE were partially miscible. The Avrami analysis was applied to analyze the nonisothermal and isothermal crystallization kinetics of the blends, the Mo Z.S. method was used to take a comparison in nonisothermal kinetics. Values of Avrami exponent indicate the crystallization nucleations of both pure PP and PP in the blends were heterogeneous, the growth of spherulites is tridimensional and the spherulites in the blends were more perfect than that in pure PP. The crystallization activation energy was estimated by Kissinger method and Arrhenius equation and the two methods draw similar results. The mLLDPE increased the crystallization rate of PP in nonisothermal crystallization process and decreased it in isothermal process. The results from nonisothermal crystallization and isothermal crystallization kinetics were not consistent because the two processes were completely different. Addition of minor mLLDPE phase favors to increase the overall crystallinity of PP, showing the mLLDPE entered the PP crystals. © 2008 Wiley Periodicals, Inc. J Appl Polym Sci 109: 1515–1523, 2008

Key words: polypropylene(PP); metallocene-catalyzed linear low density polyethylene(mLLDPE); melting behavior; crystallization kinetics; activation energy

INTRODUCTION

Polypropylene (PP) is one of the most widely used polyolefin polymers, but its application in some fields are limited due to its low fracture toughness especially at low temperature and a high notch sensitivity at room temperature. Compounding PP with a dispersed elastomeric phase [e.g., ethylene–propylene–diene rubber (EPDM)] is widely practiced,[1–5] because the rubber can increase the overall toughness of the PP matrix.[6] But the addition of elastomers often takes negative effects on some properties of PP, such as stiffness, hardness,[7] and processibility.[8]

The development of metallocene catalysts has led to production of numerous new polyolefinic materials, both in polyolefin elastomers and nonelastomers. Metallocene-catalyzed linear low density polyethylene (mLLDPE) is a kind of nonelastomeric material, due to it's low crystallinity, without double bond in molecular chain, good properties of thermal stability and aging resistance, mLLDPE can endow with higher impact strength as a modifier of PP without loss much of stiffness and processibility.[9] In addition, mLLDPE is granular form, its processing technology when blending with PP, such as extrusion and injection molding, etc., is convenient.

The physical properties of semicrystalline polymeric materials strongly depend on their crystallization and microstructure, so investigations of the crystallization behavior and crystallization kinetics of polymer blends are significant both theoretically and practically. The isothermal crystallization behavior can give useful parameters showing the grow mechanism of the spherulites, and the nonisothermal crystallization kinetics is increasing technological important because these conditions are close to practical industrial conditions. Therefore, it is highly desired to investigate the crystallization behavior and crystallization kinetics of PP/mLLDPE blends to optimize their blends composition.

In this study, the melting, crystallization behaviors, isothermal and nonisothermal crystallization kinetics were investigated with differential scanning calorimeter (DSC). The Avrami equation was applied to describe the isothermal crystallization kinetics, and the Avrami equation modified by Jeziorny, Ozawa model and the method developed by Mo were employed to describe the nonisothermal crystallization process of the PP/mLLDPE blends. The Kissinger equation and Arrhenius relation were applied to calculate the activation energy of these blends while crystallizing.

Correspondence to: J. Qin (thunder20@163.com).

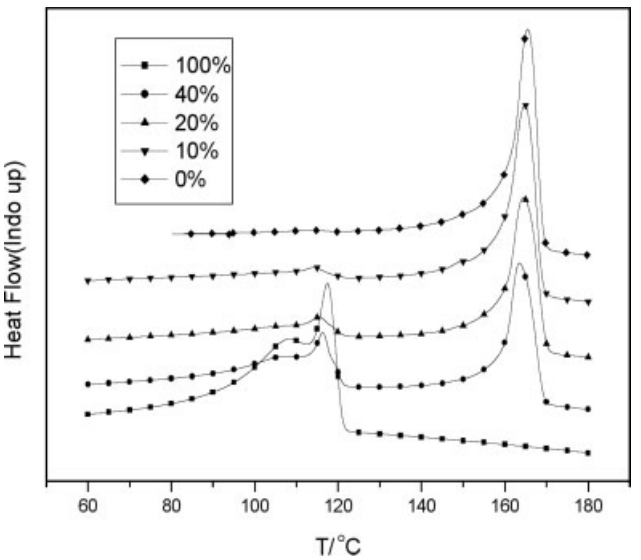

Figure 1 DSC melting curves of PP/mLLDPE blends at a heating rate of 10°C/min.

EXPERIMENTAL

Materials and sample preparation

The PP[Type K8303, melting flow index (230°C/2.16 kg) = 1.9 g/10 min] used in this study is a kind of propylene impact copolymer with 8% weight content of ethylene as a comonomer, supplied by Yanshan Petrochemical, China; The mLLDPE[type ECD342, melting flowing index (190°C/2.16 kg) = 1.0 g/10 min] sample obtained from Exxon Mobil Petrochemical.

Blends samples were prepared by melt-blending in a twin screw extruder, the temperature of each part were between 180 and 220°C. The weight ratios of mLLDPE in the blends were 0, 10, 20, 40, and 100%.

Thermal analysis

A Perkin–Elmer DSC-7 apparatus was used to record the heat flow of the blends. All the operations were carried out under a nitrogen environment. The temperature and melting enthalpy was calibrated with standard indium. Sample weights were set about 8 mg.

For melting and crystallization behaviors, samples were heated from room temperature to 200°C at a heating rate of 10°C/min and the temperature was held at 200°C for 1 min to erase thermal history. And then the melted samples were cooled to 50°C with a cooling rate of 10°C/min. As for nonisothermal crystallization, samples were heated to 200°C and held for 1 min, then cooled down to 50°C at various constant cooling rates: 2.5, 5, 7.5, 10, and 15°C/min. As for isothermal crystallization kinetics, samples were cooled from 200°C down to the required crystallization temperature (122–130°C) with a cooling rate of 150°C/min and hold for 30 min to record the heat flow. The half-time of crystallization ($t_{1/2}$) defined as the time taken for 50% crystallinity.

RESULTS AND DISCUSSION

Melting and crystallization behavior of PP/mLldpe blends

Figure 1 shows the heat flow of pure polymers and their blends at a heating rate of 10°C/min. Both the pure PP and pure mLLDPE showed two peaks in melting process. These were because the PP was made in sequential reactors and some PE segments exist in its EPR phase; and the mLLDPE is the copolymer of ethylene and other kinds of α-olefins. The two heat flow peak of PP were 114.0 and 165.5°C separately, the 114.0°C should be the melting point of PE segments. The two heat flow peaks of mLLDPE are 109.3 and 117.5°C separately. The melting temperature of PP(T_{m2}) main heat flow decreases with mLLDPE content increasing(see Table I), however, the melting peak of mLLDPE(T_{m1}) also decreases with the increasing of PP content. This observation indicates that there is some interaction between PP and mLLDPE, which is attributed to partial miscibility between molecules of PP and mLLDPE. The main heat flow peak of mLLDPE decreases shows that the main interaction of PP and mLLDPE chains exists in mLLDPE and PE segments of PP. The melting temperature (T_{m2}) of PP in the blends are between 160 and 165°C indicates that PP, both in the pure state and in the blends, exhibits only α crystal.[10,11]

The crystallization behavior were also performed by DSC at a cooling rate of 10°C/min. Figure 2 shows the crystallization exotherms of PP/mLLDPE blends compared with pure polymers respectively. All DSC traces show two crystallization peaks including those of pure polymers, indicate that these systems of blends exist two crystallizable components. The two exotherm peak of mLLDPE are 103 and 67°C separately and the 67°C should be the crystallization temperature of branches. The two exothermal peak of PP are 115.7 and 93.5°C, and there are PE segments in the PP matrix can be affirmed. The effect of mLLDPE on PP crystallizing is much similar to that of heating process, the crystallization

TABLE I
Melting Temperature (T_m) and Crystallization Temperature (T_c) of PP/mLLDPE Blends

Sample (PP/mLLDPE)	T_{m1} (°C)	T_{m2} (°C)	T_{p1} (°C)	T_{p2} (°C)
00/0	114.0	165.5	93.5	115.7
90/10	114.3	164.8	99.8	116.0
80/20	115.5	164.5	101.5	114.0
60/40	116.3	163.5	103.0	114.0
0/100	117.5		103.0	

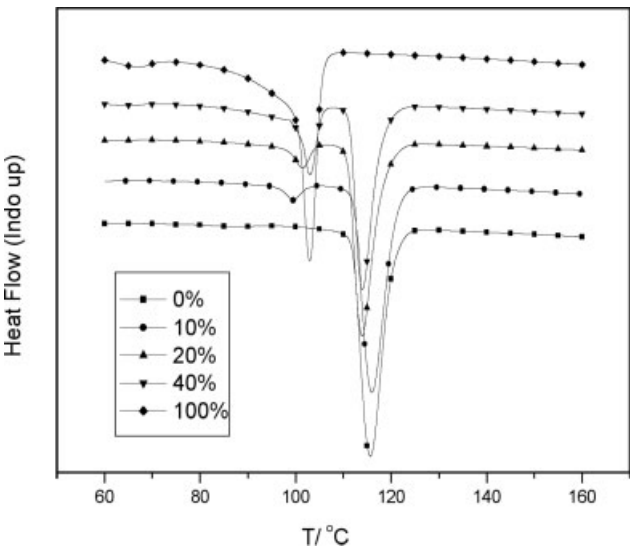

Figure 2 DSC nonisothermal crystallization curves of PP/mLLDPE blends at a cooling rate of 10°C/min.

temperature of PP matrix decrease with mLLDPE content increase, and the crystallization temperature of mLLDPE decrease with PP content increasing, also the interaction mainly exists in mLLDPE and PE segment in PP matrix.

As an example, Figure 3 shows the typical crystallization exotherms for PP in the PP/(20%) mLLDPE blend at various cooling rates. The crystallization peak temperature (T_p) for pure polymers and their blends is clearly shifted to lower temperatures as the cooling rate increasing (see Table III). The decrease of T_p with a faster cooling rate is due to the crystallization rate is lower than the experimental cooling rate.[12] At a slower cooling rate, PP molecules have enough time to form the necessary nuclei for crystallization and, therefore, come to a higher T_p.

For all the samples, sample crystallinity (X_{PP}) is defined as:

$$X_{PP} = \frac{\Delta H_C}{\Delta H_C^O} \tag{1}$$

where ΔH_C^O = 187.7 (J/g), which is the 100% crystallization enthalpy of PP.[13] About 187.7 (J/g) is the 100% crystallization enthalpy of PP,[13] ΔH_c is the crystallization enthalpy of PP in the pure PP or the PP/mLLDPE blends. The X_{PP} values of isothermal and nonisothermal crystallization processes were listed in Tables II and Table III seperately. The Xpp of PP/mLLDPE is higher than that of pure PP, showing the mLLDPE chains entered the PP crystals. This is another proof showing miscibility of PP and mLLDPE.

Isothermal crystallization kinetics

Up to date, several analytical methods have been developed to describe the crystallization kinetic of polymers: (i) Avrami analysis,[14–19] (ii) Ozawa analysis,[20,21] (iii) Ziabicki analysis,[22,23] and (iv) others,[24–27] such as Mo Z.S. analysis. In this article, the Avrami analysis was used to describe the crystallization kinetics of PP/mLLDPE blends and Mo Z.S. analysis was taken as a contrastive study.

The Avrami equation[14–16,19,28,29] has been widely used to describe isothermal crystallization kinetics of polymers:

$$1 - X_t = exp(-kt^n) \tag{2}$$

where X_t is the relative crystallinity, k is the growth rate constant and n is the Avrami exponent. Here, the value of Avrami exponent n depends on the nucleation mechanism and growth dimension; the parameter k is a function of the nucleation and the growth rate. The relative crystallinity X_t, as a function of crystallization time is defined as:

$$X_t = \frac{\int_0^t (dH/dt)dt}{\int_0^\infty (dH/dt)dt} \tag{3}$$

where dH/dt is the rate of heat evolution; t_0 and t_∞ were the time at which crystallization starts and ends, respectively.

Figure 4 shows the DSC traces for PP/mLLDPE blend that had been isothermally crystallized at different temperatures. And Figure 5 shows the relative crystallinity of PP/(20%) mLLDPE blends at various crystallization temperatures. All curves in Figure 5 show a sigmoidal shape. The plot of X_t versus t shifts to the right with the crystallization tempera-

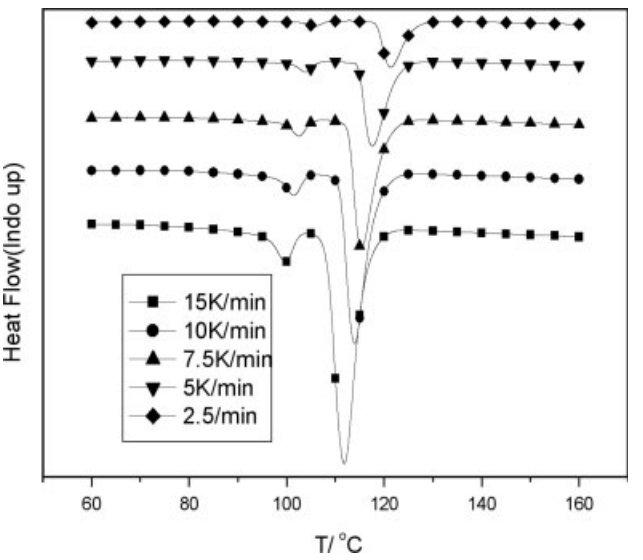

Figure 3 DSC nonisothermal crystallization curves for PP in the PP/(20%) mLLDPE blends at various cooling rates.

TABLE II
Isothermal Crystallization Parameters of PP/mLLDPE Blends at Different Crystallization Temperatures

Sample mLLDPE (%)	T (°C)	n	log k	$t_{1/2}$ (min)	X_{PP} (%)	E_a (kJ/mol)
0	122	2.33	−0.090	0.93	36.548	−251.4
	124	2.44	−0.625	1.54	39.478	
	126	2.28	−1.10	2.61	41.609	
	128	2.18	−1.60	4.71	42.355	
	130	2.15	−2.10	8.15	40.224	
	122	2.35	−0.139	1.03	41.156	
	124	2.54	−0.782	1.77	42.888	
20	126	2.82	−1.49	2.99	43.147	−332.3
	128	2.95	−2.17	4.81	44.286	
	130	3.05	−2.85	7.65	44.153	
	122	2.54	−0.481	1.35	44.575	
	124	2.61	−1.02	2.15	44.752	
40	126	2.79	−1.70	3.60	46.351	−313.2
	128	2.89	−2.34	5.75	45.818	
	130	2.99	−3.01	9.02	43.776	

ture increases, showing the decrease of crystallization rate, indicating the crystallization is enhanced as temperature decreases, the crystallization half-time $t_{1/2}$ can be calculated directly from the relative crystallinity versus time plot. That is also because of the strong temperature dependence of the nucleation and the growth parameters.[30]

Rewritten eq. (2) in a double logarithm form:

$$\log[-\ln(1 - X_t)] = \log(k) + n\log(t) \quad (4)$$

then, the Avrami parameters can be estimated from the slope and intercept of $\log[-ln(1 - X_t)]$ versus log$t$ according to eq. (4). Figure 6 shows the plot of $\log[-ln(1 - X_t)]$ versus log$t$ for isothermal crystallization of PP/(20%)mLLDPE blends. Each curve shows good linear relationship indicating that the Avrami equation can properly describe the isothermal crystallization behavior of these samples. All lines in Figure 6 are straight and almost paralleled to each other, shifting to less time with decreasing temperature. The Avrami parameters estimated from the plot of $\log[-ln(1 - X_t)]$ versus log$t$ are listed in Table II.

The n values of PP increase and then decrease with increasing of crystallization temperature within 2.15–2.44, and that of the PP/mLLDPE blends increase with increasing of crystallization temperature from 2.35–3.05. The differences between pure PP and PP/mLLDPE blends are the dilution effect and high mobility of mLLDPE at crystallization temperatures help PP to form compact crystals or spherulites. The values of Avrami parameters showed the nucleation mechanism of both PP and PP/mLLDPE blends are heterogeneous, and the increasing of Avrami parameters means more perfection of the spherulites. The crystallinity of PP/mLLDPE blends are higher than pure PP, shows the mLLDPE chains enter to the PP crystals.

In Table II, the crystallinity of the both PP and PP/mLLDPE blends increase and then decrease with

TABLE III
Nonisothermal Crystallization Parameters of PP/mLLDPE Blends at Different Cooling Rates

Sample mLLDPE (%)	D (°C/min)	n	log k'	$t_{1/2}$ (min)	T_p (°C)	X_{PP} (%)
0	2.5	5.64	−1.29	3.5	121.7	44.0
	5.0	5.60	−0.34	1.87	119.0	43.5
	7.5	5.65	−0.12	1.37	117.3	43.2
	10	5.39	−0.027	1.05	115.7	43.0
	15	4.60	0.045	0.66	113.3	42.0
	2.5	4.88	−1.05	3.23	121.3	46.1
	5.0	5.52	−0.36	1.98	117.5	45.3
20	7.5	6.40	−0.17	1.52	115.3	45.0
	10	6.33	−0.067	1.13	114.0	44.3
	15	5.75	0.044	0.72	111.8	43.0
	2.5	4.87	−1.03	3.15	121.0	47.6
	5.0	5.47	−0.32	1.83	117.3	46.9
40	7.5	6.07	−0.11	1.30	115.3	46.0
	10	6.39	−0.014	1.0	114.0	45.0
	15	6.00	0.062	0.66	112.0	43.7

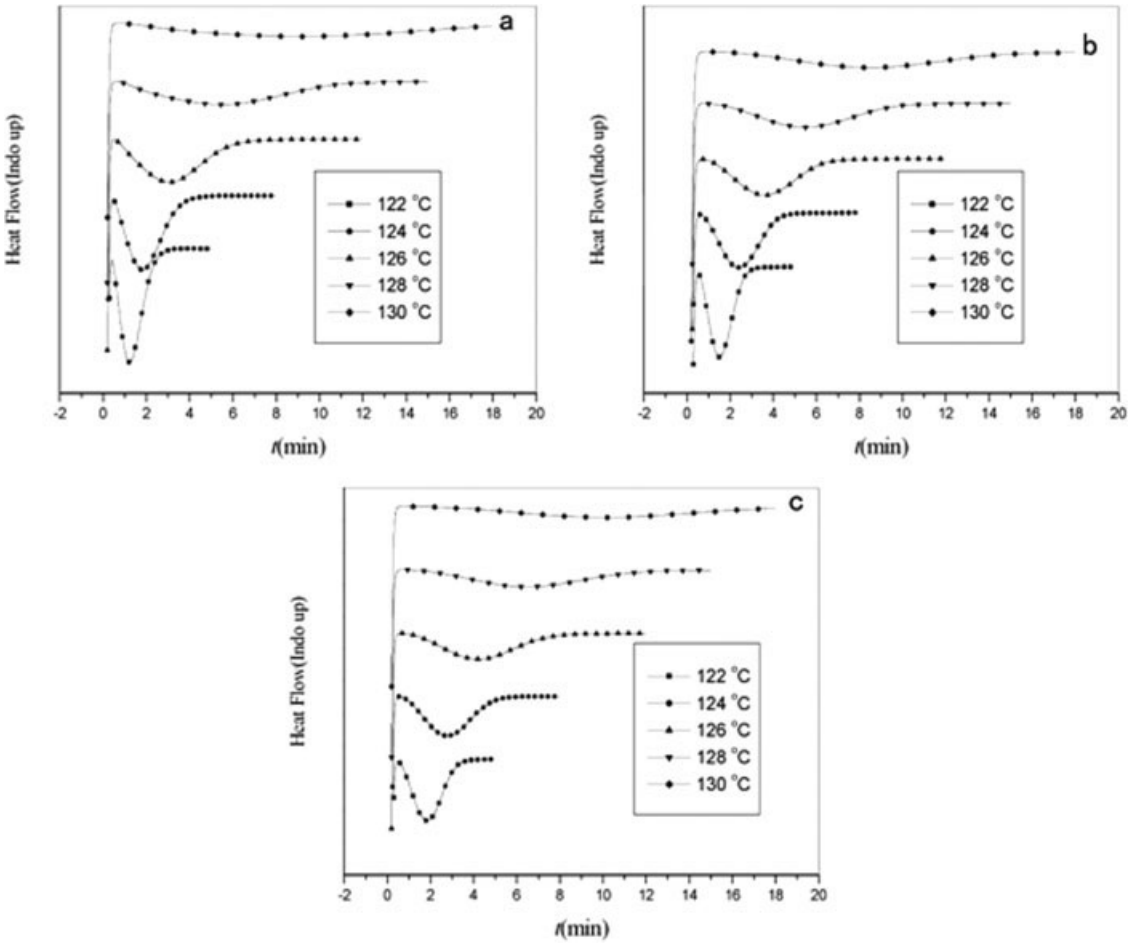

Figure 4 DSC isothermal crystallization curves for PP in the PP/mLLDPE blends at various crystallization temperatures (a, 0%; b, 20%; c, 40%).

increasing of crystallization temperature. These results show that the mobility of PP chains increase but crystallization rate decrease with increasing temperature. At high temperatures, the mobility of PP chains is too high to crystallize and the crystallinity decrease.

However, the crystallization rate is dependent on the blend composition and temperature. On one hand, for the pure PP, the crystallization rate constant (k') decreases with increasing temperature, and the crystallization half-time ($t_{1/2}$) increases (see Table II). Similar trends in both the k' and $t_{1/2}$ are observed for the PP/(20%)mLLDPE and PP/(40%)mLLDPE blends. On the other hand, at the same temperature, the k' slightly decreases with the mLLDPE content increase, and the $t_{1/2}$ adversely affected because the mLLDPE lengthened the distance from the chains to growing crystal.

Nonisothermal crystallization kinetics

The Avrami equation can be modified to describe nonisothermal crystallization.[17–18,31,32] For nonisothermal crystallization at a chosen cooling rate, the relative crystallinity X_t is a function of crystallization temperature. That is, eq. (3) can be rewritten as follows:

$$X_t = \frac{\int_0^T (dH/dT)dT}{\int_0^\infty (dH/dT)dT} \tag{5}$$

where T is the crystallization temperature, T_0 and T_∞ represents the onset and end temperature of crystallization, respectively.

As an example, Figure 7 shows the relative crystallinity of PP in the PP/(20%)mLLDPE blends at various cooling rates. All curves in Figure 7 show a reversed sigmoidal shape, indicating a fast primary process during the initial stages and slower secondary process during the later stages. The plot of X_t versus T shifts to the low temperature region as the cooling rate increases. The lower cooling rate provides more fluidity and diffusivity for the molecules due to relative lower viscosity and more time to crystallize, thus inducing higher crystallinity and

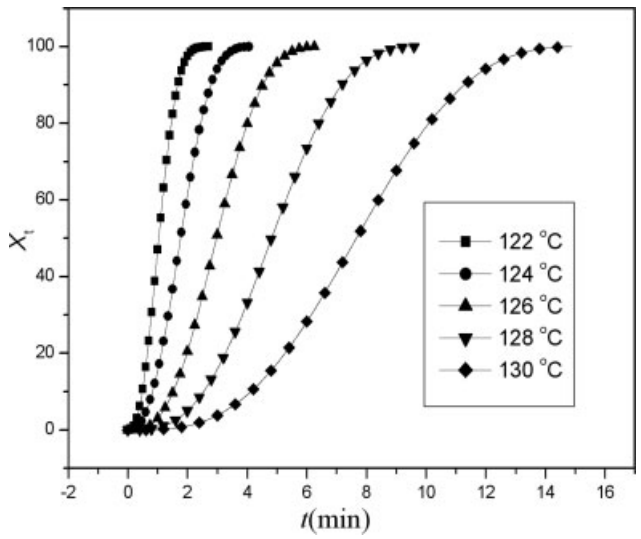

Figure 5 Plot of relative crystallinity X_t versus crystallization time t for PP in the PP/(20%) mLLDPE blends at various crystallization temperatures.

more perfect crystallization at lower cooling rates, as shown in Table III.

The crystallization temperature can be converted to crystallization time t using a equation.[23,32]

$$t = \frac{T_0 - T}{D} \tag{6}$$

where D is the cooling rate. Using eq. (5) the temperature axis in Figure 7 can be transformed into time scale, as shown in Figure 8. The sigmoidal shape of the curves suggests the modified Avrami analysis is applicable for nonisothermal crystallization of PP/mLLDPE blends. Meanwhile, the crystallization half-time $t_{1/2}$ can be calculated directly from the relative crystallinity versus time plot,[19,33] as shown in Table III.

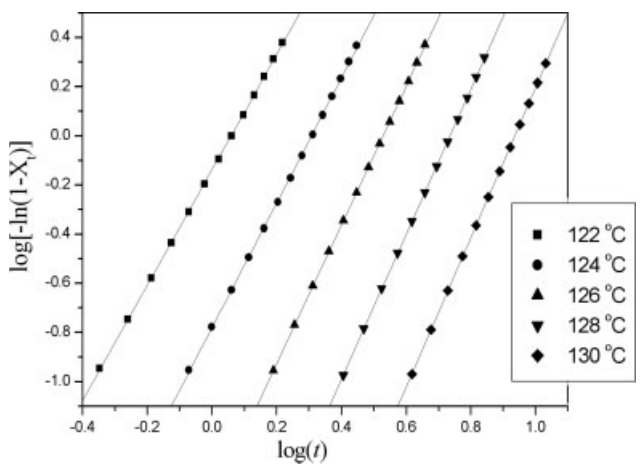

Figure 6 Avrami plot of PP in the PP/(20%) mLLDPE blends at various crystallization temperatures.

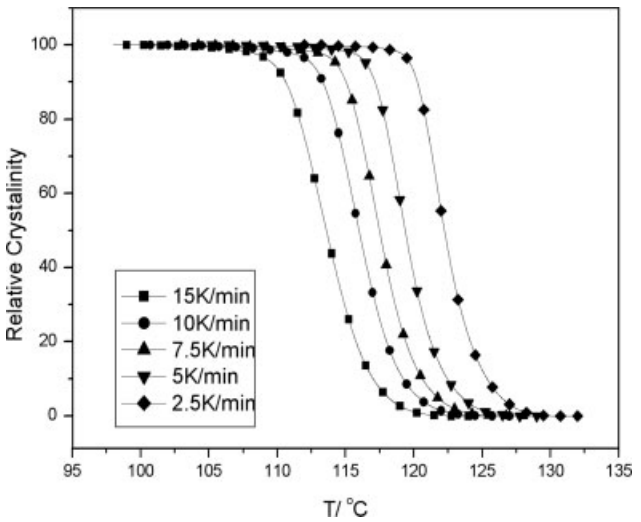

Figure 7 Plot of relative crystallinity X_t versus crystallization temperature T of PP/(20%) mLLDPE blends at various cooling rates.

Figure 9 shows the Avrami plot of $\log[-\ln(1 - X_t)]$ versus $\log t$ for nonisothermal crystallization of PP/(20%) mLLDPE blends. All lines in Figure 9 are straight and almost paralleled implies that the nucleation mechanism and crystal growth geometries are similar, although the cooling rates are different. The Avrami parameters are estimated from the plot of $\log[-\ln(1 - X_t)]$ versus $\log t$, and the values are listed in Table III. Regardless of the cooling rates, the Avrami exponent n for the pure PP is in the range of 4.60–5.65, compare to the literature data under nonisothermal conditions.[34] The Avrami exponents for the PP/mLLDPE blends are in the rage of 4.87–6.40, regardless of the blend composition and cooling rates, suggesting the mLLDPE help PP form

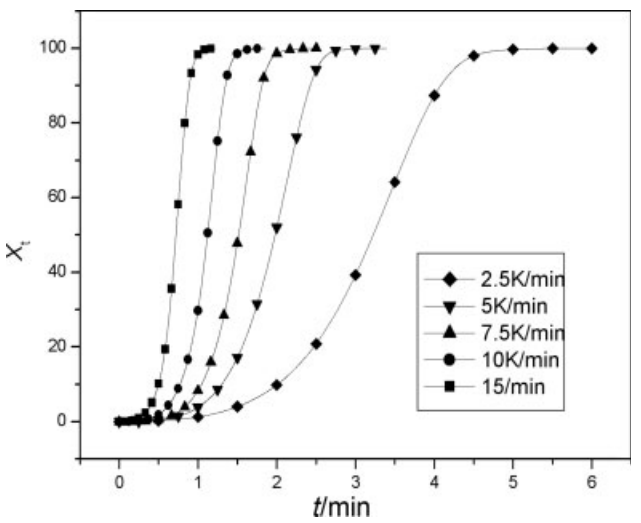

Figure 8 Plot of relative crystallinity X_t versus crystallization time t for PP in the PP/(20%) mLLDPE at various cooling rates.

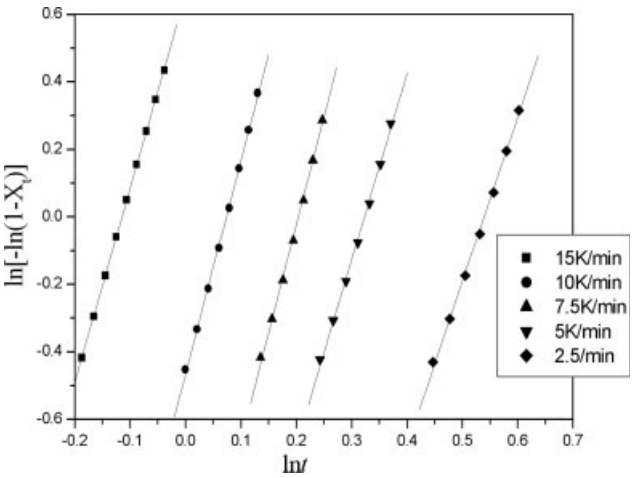

Figure 9 Avrami plot for PP in the PP/(20%)mLLDPE blends at various cooling rates.

more perfect spherulites, and this result consistent with isothermal crystallization process. But the Avrami exponents deduced from nonisothermal crystallization are not exact because the temperatures of nonisothermal crystallization are changing continuously, and the crystallization rate constant k for nonisothermal crystallization should be corrected as follows[32]: $\log k' = \log k/\mathrm{D}$.

As a result, the crystallization rate (k') increase with cooling rate, and the crystallization half-time ($t_{1/2}$) decreased (see Table III). The k' and the $t_{1/2}$ changed a little with the mLLDPE content increasing compare with isothermal crystallization, because the mLLDPE acts as a diluter and lengthened the distance at the same time, and the two effects are contradict.

For comparison, a new simple method which is proposed by Mo and coworkers,[24] is employed as follows:

$$\log D = \log F(T) - a \log t \tag{7}$$

where $F(T) = [K(T)/k]^{1/m}$ refers to the cooling rate value which must be chosen within unit crystallization time when the measured system amounts to a certain relative crystallinity, then the $F(T)$ value has a definite physical and practical meaning, that is, at a certain relative crystallinity, a high value of $F(T)$ means a high cooling rate is needed to reach this X_t in a unit time, which reflects the difficulty of its crystallization process; a is the ratio of the Avrami exponent n to the Ozawa exponent m(a = n/m). According to eq. (7), $F(T)$ and a can be determined from the slope and intercept of logarithm plot of cooling rate versus time at different relative crystallinity (X_t)of 20, 30,40, 50, and 60%, respectively. Figure 10 presents the result of PP/(20%)mLLDPE blends. Good fitness of the lines shows the new method is successful for describing the nonisothermal crystallization process of PP/mLLDPE blends. The values of $F(T)$ and a for all the samples are listed in Table IV The $F(T)$ values increase with the relative crystallinity for the same blend. However, at the same relative crystallinity, the values of $F(T)$ of PP are lower than that of PP/mLLDPE blends, implying the faster crystallization of PP than that of PP/mLLDPE blends. This conclusion is not well consistent with the results obtained from modified Avrami analysis, because the addition of mLLDPE obviously lowered the crystallization temperatures of the blends, and the crystallization rates are not only determined by crystallization rate, but also temperature. The values of a are almost a constant for a given composition at different relative crystallinity, and the a values of PP/(20%)mLLDPE are larger than that of others, indicating that the interaction between PP and mLLDPE is most obvious and a certain mass ratio.

The effect of mLLDPE on PP are not the same in isothermal and nonisothermal crystallization kinetics. At high temperatures (isothermal processes), the mLLDPE lengthens the distances of PP chains to nuclei and then decreases the crystallization rate. But at lower temperatures (nonisothermal processes), the mLLDPE increases the mobility of PP chains and then increases crystallization rate.

Activation energy for crystallization

The activation energy for isothermal crystallization can be approximately described by the Arrhenius equation.[35,36,16]

$$k^{1/n} = k_0 \exp\left(-\frac{E_a}{RT_c}\right) \tag{8}$$

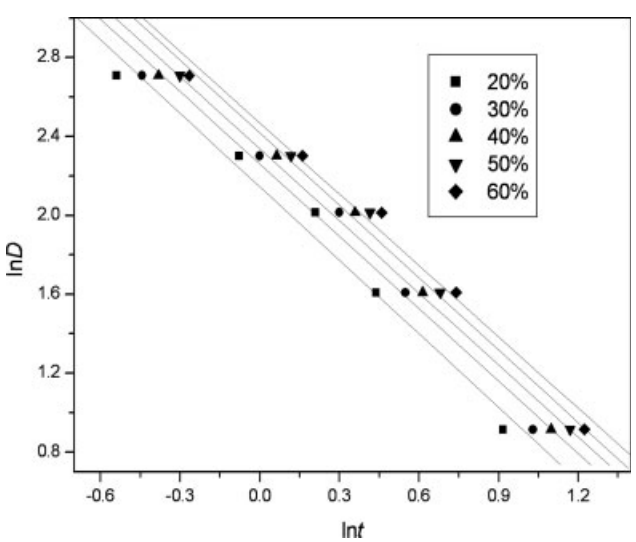

Figure 10 Mo plot for PP in the PP/(20%)mLLDPE blends at different relative crystallinity.

TABLE IV
Nonisothermal Crystallization Parameters of PP/mLLDPE Blends at Different Relative Crystallinity

Sample (mLLDPE%)	X_t (%)	$F(t)$	a	E_a (kJ/mol)
0	20	3.41	1.093	−300.6
	30	3.78	1.081	
	40	4.10	1.086	
	50	4.37	1.092	
	60	4.62	1.094	
20	20	3.71	1.246	
	30	4.17	1.222	−245.5
	40	4.50	1.218	
	50	4.88	1.224	
	60	5.13	1.205	
40	20	3.81	1.093	
	30	4.27	1.087	−258.7
	40	4.55	1.074	
	50	4.86	1.085	
	60	5.18	1.094	

The slope of the Arrhenius plot of (1/n)ln$k$ versus $1/T_c$ determines E_a/R, as shown in Figure 11. The value of the activation energy is found to be −251.4 kJ/mol for PP melt crystallization, −332.3 and −313.2 kJ/mol for PP/(20%)mLLDPE and PP/(40%)mLLDPE separately (Table II).

For nonisothermal crystallization, the crystallization activation energy E_a can be estimated from the variation of crystallization peak temperature T_p with cooling rate D by the Kissinger approach.[37]

$$\frac{d[\ln(D/T_p^2)]}{d(1/T_p)} = -\frac{E_a}{R} \tag{9}$$

where R is the universal gas constant.

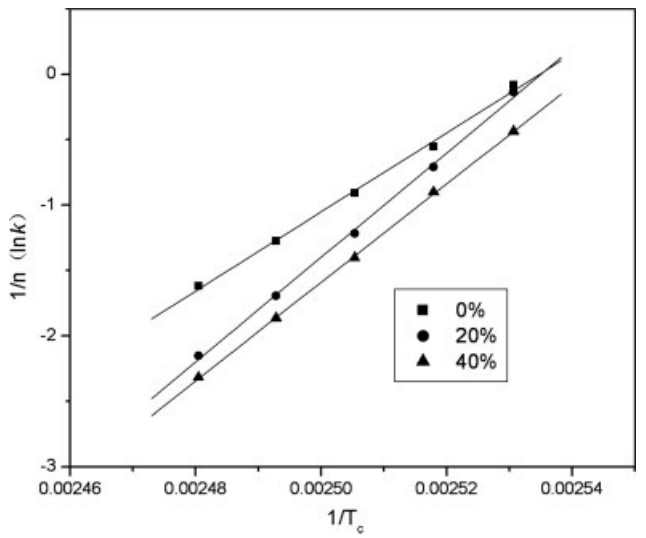

Figure 11 Arrhenius plot of (1/n)ln$k$ versus $1/T_c$ of PP/mLLDPE blends for isothermal crystallization at different mLLDPE content.

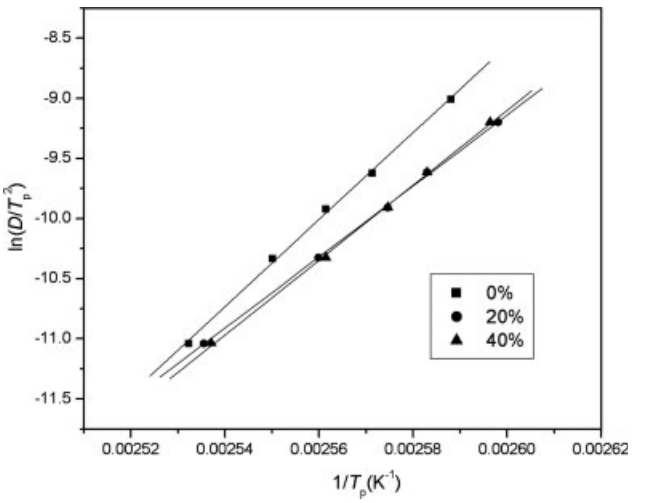

Figure 12 Kissinger plot of $ln(D/T_p^2)$ versus $1/T_p$ of PP/mLLDPE blends for nonisothermal crystallization at different mLLDPE content.

The Kissinger plot, that is the plot of $ln(D/T_p^2)$ versus $1/T_p$ for PP/mLLDPE blends, is shown in Figure 12. The E_a is estimated to be −300.6 kJ/mol for pure PP, −245.5 kJ/mol for the PP/(20%)mLLDPE blends and −258.7 kJ/mol for PP/(40%)mLLDPE blends (See Table IV).

The E_a values ranges are close to each other, showing the Kissinger approach and Arrhenius equation have the similar effect in evaluating E_a values.

CONCLUSIONS

The melting behaviors and crystallization kinetics of PP/mLLDPE were investigated with DSC. The result showed that there are interactions between PP and mLLDPE chains mainly exist in mLLDPE and PE segment in PP matrix. The crystallinity of the blends increase with the increasing of mLLDPE content showing mLLDPE entered the PP crystal. The crystallization kinetics of the blends was investigated fairly well by both Avrami and Mo Z.S. analysis. The values of the Avrami exponent derived from isothermal crystallization show the nucleation mechanism are heterogeneous. The values of the Avrami exponent of PP are lower than that of PP/mLLDPE blends shows mLLDPE help PP to form perfect spherulites. At the same cooling rate, crystallization rate increased with increasing mLLDPE content. But at the same temperature, the crystallization rate decreased with increasing mLLDPE content, because the mLLDPE shifts the crystallization temperature to lower temperature. The crystallization activation energy derived from Kissinger analysis and Arrhenius equation are close showing the two methods have the similar effect in evaluating E_a values.

References

1. Karger-Kocsis, J.; Kalló, A.; Kuleznev, V. N. Polymer 1984, 25, 279.
2. Coppola, F.; Greco, R.; Martuscelli, E.; Kammer, H. W. Polymer 1987, 28, 47.
3. Tam, W. Y.; Cheung, T.; Li, R. K. Y. Polym Test 1996, 15, 452.
4. Van der Wal, A.; Mulder, J. J.; Oderkerk, J.; Gaymans, R. J Polymer 1998, 39, 6781.
5. Yokoma, Y.; Ricco, T. J Appl Polym Sci 1997, 66, 1007.
6. Karger-Kocsis, J. Polypropylene-Structure, Blends and Composites; Chapman & Hall: London, 1994.
7. Qiu, G. X.; Raue, F.; Ehrenstein, G. W. J Appl Polym Sci 2002, 83, 3029.
8. Wang, D.; Gao, J.; Li, S. China Plast 2003, 17, 19.
9. Qin, J.-L.; Gao, J.-G. China Plast 2004, 18, 21.
10. Shieh, Y. T.; Lee, M. S.; Chen, S. A. Polymer 2001, 42, 4439.
11. Ha, C. S.; Kim, S. C. J Appl Polym Sci 1988, 35, 2211.
12. Park, J. Y.; Kwon, M. H.; Park, O. O. J Polym Sci Part B: Polym Phys 2000, 38, 3001.
13. Kirshenbaum, I.; Wilchinsky, Z. W.; Groten, B. J Appl Polym Sci 1964, 8, 2723.
14. Zhang, X.; Xie, T.; Yang, G. Polymer 2006, 47, 116.
15. Lu, X. F.; Hay, J. N. Polymer 2001, 42, 9423.
16. Li, C.; Tian, G.; Zhang,Y.; Zhang, Y. Polym Test 2002, 21, 919.
17. Herrero, C. H.; Acosta, J. L. Polymer 1994, 26, 786.
18. De Juana, R.; Jauregui, A.; Calahora, E.; Cortazar, M. Polymer 1996, 37, 3339.
19. Lee, S. W.; Ree, M.; Park, C. E.; Jung, Y. K.; Park, C. S.; Jin, Y. S.; Bae, D. C. Polymer 1999, 40, 7137.
20. Ozawa, T. Polymer 1971, 12, 150.
21. Ozawa, T. Polymer 1978, 19, 1142.
22. Ziabicki, A. Coll Polym Sci 1974, 6, 252.
23. Ziabicki, A. Appl Polym Symp 1967, 6, 1.
24. Liu, T. X.; Mo, Z. S.; Wang, S. E.; Zhang, H. F. Polym Eng Sci 1997, 37, 568.
25. Caze, C.; Devaux, E.; Crespy, A.; Cavrot, J. P. Polymer 1997, 38, 497.
26. Nakamura, K.; Katayama, K.; Amano, T. J Appl Polym Sci 1973, 17, 1031.
27. Chan, T. W.; Isayev, A. I. Polym Eng Sci 1994, 34, 461.
28. Avrami, M. J Chem Phys 1939, 7, 1103.
29. Avrami, M. J Chem Phys 1940, 8, 212.
30. Seo, Y. S.; Kim, J. H.; Kin, K. U.; Kim, Y. C. Polymer 2000, 41, 2639.
31. Tobin, M. C. J Polym Sci Part B: Polym Phys 1974, 12, 399.
32. Jeziorny, A. Polymer 1978, 19, 1142.
33. Xu, W. B.; Ge, M. L.; He, P. S. J Appl Polym Sci 2001, 82, 2281.
34. Xu, W. B.; Ge, M. L.; He, P. S. Acta Polym Sin 2001, 5, 584.
35. Cebe, P.; Hong, S. D. Polymer 1986, 27, 1183.
36. Villanova, P. C.; Ribas, S. M.; Guzman, G. M. Polymer 1985, 26, 423.
37. Kissinger, H. E. J Res Natl Bur Stds (US) 1956, 57, 217.